



CrossMark  
 click for updates

Cite this: *RSC Adv.*, 2015, 5, 24788

# A zinc sulfide-supported iron tetrakis (4-carboxyl phenyl) porphyrin catalyst for aerobic oxidation of cyclohexane

Yue-xiu Jiang, Tong-ming Su, Zu-zeng Qin\* and Guan Huang\*

Zinc sulfide-supported iron tetrakis (4-carboxyl phenyl) porphyrin (Fe TCPP/ZnS) was prepared and used for aerobic cyclohexane oxidation. X-ray diffraction, ultraviolet-visible spectroscopy and Fourier-transform infrared spectroscopy were carried out. The effects of oxygen pressure, reaction temperature, amount of iron tetrakis (4-carboxyl phenyl) porphyrin (Fe TCPP) and reaction time on the Fe TCPP/ZnS-catalyzed cyclohexane oxidation process were investigated. Fe TCPP/ZnS exhibited excellent activity for aerobic cyclohexane oxidation. Under optimal reaction conditions, the turnover number, cyclohexane conversion, cyclohexanone and cyclohexanol yields were  $8.6 \times 10^5$ , 64.9% and 24.4%, respectively. The stability of Fe TCPP was improved after immobilization on zinc sulfide (ZnS), and the catalyst maintained nearly original levels of activity after several reaction cycles.

Received 8th December 2014  
 Accepted 2nd March 2015

DOI: 10.1039/c4ra15991h

[www.rsc.org/advances](http://www.rsc.org/advances)

## Introduction

Selective cyclohexane oxidation is of great significance for chemical industries, because the products of the reaction, cyclohexanone and cyclohexanol, are important intermediates in the manufacture of nylons 6 and 66.<sup>1</sup> The commercial process for cyclohexane oxidation is carried out at 413–443 K and 1.0–2.0 MPa and affords only 4% cyclohexane conversion.<sup>2</sup> Considering this low conversion and the fact that the process promotes severe issues, such as corrosion and pollution, developing highly effective and environment-friendly heterogeneous catalysts for cyclohexane oxidation remains an urgent necessity. In catalytic oxidation of cyclohexane by  $\text{FeP}(\text{PF}_6)_4$ ,  $\text{FePCL}_4$ ,  $\text{FeP-NaYimp}$ , and  $\text{Fe-NaY}$ , the cyclohexanol yields reach 30%, 15%, 25%, and 38%, respectively.<sup>3</sup> However, the activity and stability of the catalyst should be further improved.

Metalloporphyrins, as model catalysts of cytochrome P-450, have recently been recognized as a valuable biomimetic catalysts for alkane oxidation and many other oxidation reactions with high selectivity and efficiency.<sup>4–7</sup> However, metalloporphyrins are unstable, difficult to reuse, and degrade easily in the presence of inert substrates,<sup>8</sup> which limits their practical application in industrial processes. These disadvantages can be overcome by immobilization on supports. Many supports can provide a suitable micro-environment for various reactions and site isolation of metalloporphyrins, reduce the formation of catalytically inactive  $\mu$ -oxo porphyrin dimers, and increase the

stability of porphyrins toward the oxidant.<sup>9</sup> To improve the catalytic performance of the metalloporphyrins, immobilization of metalloporphyrins on chitosan,<sup>10</sup> organosilicon,<sup>11</sup> boehmite,<sup>9,12</sup> halloysite,<sup>13</sup> zinc hydroxide nitrate,<sup>14</sup> ferroferric oxide,<sup>15</sup> polymeric microspheres,<sup>16,17</sup> micro and mesoporous supports,<sup>18</sup> porous metal-organic frameworks,<sup>19</sup> and some other supports<sup>20–23</sup> has been investigated.

Carbon nanotube-supported iron porphyrins<sup>24</sup> and boehmite-supported iron tetraphenylporphyrins<sup>12</sup> are conventionally prepared after iron porphyrins immobilization on carbon nanotubes or boehmite to improve the performance of the porphyrins. And from the previous study, we found that the stability and catalytic activity of the metalloporphyrin can be enhanced when used chitosan or boehmite as the support.<sup>8,9,12,25,26</sup> However, cyclohexane conversion, cyclohexanone and cyclohexanol yields remain very low. As such, finding new supports which can significantly improve the cyclohexanone and cyclohexanol yields catalyzed by iron porphyrins is necessary. Zinc sulfide (ZnS) materials are promising supports because they are chemically more stable and technologically more advanced than other chalcogenides. These materials have been used as supports to promote electron transfer reactions at lower potentials and catalyze electrochemical oxidation of enzymes to thiocholine.<sup>27</sup> However, the use of ZnS as metalloporphyrins supports has not been reported.

In this study, zinc sulfide-supported iron tetrakis (4-carboxyl phenyl) porphyrin (Fe TCPP/ZnS) was initially prepared and used for the aerobic oxidation of cyclohexane to cyclohexanone and cyclohexanol. Fe TCPP/ZnS was characterized by X-ray diffraction (XRD), ultraviolet-visible spectroscopy (UV-vis), Fourier-transform infrared (FT-IR) spectroscopy, and X-ray photoelectron spectrometer (XPS). The effects of oxygen

Guangxi Key Laboratory of Petrochemical Resource Processing and Process Intensification Technology, School of Chemistry and Chemical Engineering, Guangxi University, Nanning 530004, PR China. E-mail: qinzuzeng@gmail.com; huanggg66@126.com; Fax: +86 771 3233718; Tel: +86 771 3233718

pressure, reaction temperature, amount of Fe TCPP and reaction time on the Fe TCPP/ZnS-catalyzed cyclohexane oxidation process, as well as the reuse of catalysts for cyclohexane oxidation were investigated. This study developed an efficient catalyst consisting of iron porphyrin immobilized on ZnS. The catalysts obtained displayed excellent cyclohexanone and cyclohexanol yields during cyclohexane oxidation.

## Experimental section

### Preparation of TCPP catalysts

A total of 2.22 g (0.0148 mol) of 4-carboxybenzaldehyde and 70 mL of propionic acid were added to a 250 mL three-necked, round-bottomed flask with stirring at a speed of 100 rpm. Upon complete dissolution of 4-carboxybenzaldehyde, the solution was heated to reflux the propionic acid. Then 1.02 mL (0.0148 mol) of pyrrole was dropped slowly into the solution using a funnel. After refluxing in the dark for 1 h, the solution was cooled to room temperature and filtered. The filtered cake was vacuum dried after washing with deionized water and TCPP was obtained.

### Preparation of Fe TCPP catalysts

TCPP (0.5 g) and *N,N*-dimethyl formamide (80 mL) were added to a 250 mL three-necked, round-bottomed flask with stirring at a speed of 100 rpm. Upon complete dissolution of TCPP, the solution was heated to reflux and 1.5 g of  $\text{FeCl}_2 \cdot 4\text{H}_2\text{O}$  was added to the mixture. Refluxing was continued for 1 h, and the reaction process was tracked using a thin layer chromatography plate. After completion of the reaction, the temperature of the reaction solution was cooled to below 100 °C. Hydrochloric acid ( $6.0 \text{ mol L}^{-1}$ ) was dropped slowly into the solution until complete dissolution of the red solid. The solution was cooled to room temperature and 100 mL of deionized water was added to it. The solution was then allowed to stand for one night and filtered. The filtered cake was vacuum dried after washing with deionized water and Fe TCPP was obtained.

### Preparation of Fe TCPP/ZnS catalysts

A total of 200 mL of  $1.3 \text{ mol L}^{-1} \text{Na}_2\text{S}$  solution was slowly added to 200 mL of  $1.3 \text{ mol L}^{-1} \text{ZnSO}_4$  solution with stirring to yield a white precipitate. The precipitate was filtered and washed with distilled water until  $\text{SO}_4^{2-}$  ion were no longer detected in the washings; here,  $0.05 \text{ mol L}^{-1} \text{BaCl}_2$  solution was used as a detector. The precipitate was added then to ethanol (150 mL) in a three-necked flask, and the mixture was stirred at high speed for 0.5 h. A solution of Fe TCPP (25 mg) in absolute ethanol (20 mL) was slowly added to the suspension, and the mixture was heated at 65 °C with rapid stirring for 5 h. The suspension was filtered, and the solid was washed with distilled water. The filtered cake was dried at 0.09 MPa and 160 °C for 5 h and Fe TCPP/ZnS was obtained.

### Cyclohexane oxidation catalyzed by Fe TCPP/ZnS with $\text{O}_2$

A 250 mL autoclave reactor was charged with a measured amount of Fe TCPP or Fe TCPP/ZnS and cyclohexane (200 mL).

The mixture was stirred at 300 rpm and heated to 145–175 °C.  $\text{O}_2$  was continuously pumped into the reaction system and the pressure was kept at 0.6–1.1 MPa.  $\text{O}_2$  flow was measured with a rotameter, and the tail gas was determined with a digital oxygen detector. Gas chromatography was used to analyze reaction mixture samples using an internal standard method with chlorobenzene as the standard substance. To study the subsequent reuse of Fe TCPP/ZnS, the catalysts were separated from the reaction mixture immediately after use, dried naturally at room temperature, and used in the next catalytic cyclohexane oxidation reaction.

### Characterization of Fe TCPP/ZnS catalysts

XRD patterns of ZnS and Fe TCPP/ZnS were obtained using a D/MAX-2600/PC X-ray powder diffraction instrument (Rigaku Corporation), equipped with a Cu  $K\alpha$  radiation source. UV-vis spectra of supported and unsupported catalysts in dimethyl formamide were recorded using a UV-2102 PCS spectrometer (Shanghai Nylon Co., Ltd.). FT-IR spectra of ZnS and Fe TCPP/ZnS were recorded on a Nexus 470 FT-IR spectrophotometer (Nicolet Instrument Corp.) from  $400 \text{ cm}^{-1}$  to  $4000 \text{ cm}^{-1}$ ; KBr was used as the background. The oxidation state and surface composition were analyzed using an X-ray photoelectron spectrometer (XPS) (Kratos Ultra Axis DLD), equipped with an Al  $K\alpha$  radiation source, at 150 W with a pass energy of 40 eV.

## Results and discussion

### Characterization of Fe TCPP/ZnS material

When Fe TCPP was anchored on white ZnS, a light green solid was obtained. This indicates that the presence of Fe TCPP on the ZnS. On the XRD patterns of ZnS and Fe TCPP/ZnS (Fig. 1), characteristic diffraction peaks of ZnS were found at 28.56°, 47.50°, and 56.37°; these peaks indicate that the support has a cubic lattice structure (JCPDS 05-0566).<sup>28</sup> The diffraction peaks of Fe TCPP/ZnS were similar to those of ZnS because of the low content of immobilized Fe TCPP in the former. This result indicates that Fe TCPP immobilization does not change the crystal structure of ZnS, which favors Fe TCPP immobilization on the ZnS surface.

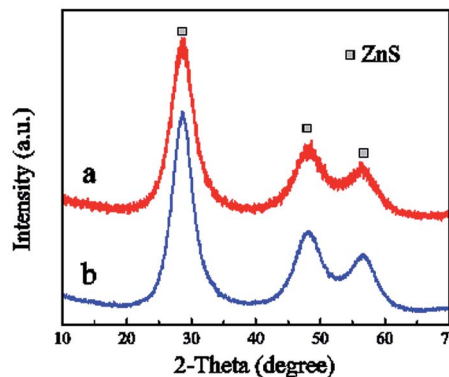


Fig. 1 XRD patterns of ZnS (a) and Fe TCPP/ZnS (b).

Fig. 2 shows the UV-vis spectra of Fe TCPP and Fe TCPP/ZnS. The Soret peak of Fe TCPP at room temperature was observed at 418 nm. After Fe TCPP immobilization on ZnS, the Soret peak violet shifted to 415 nm and a new peak was observed at 460 nm, which may be explained by interactions between the metal-porphyrin complex and the surface of the solid support. This finding indicates that Fe TCPP is immobilized on ZnS through coordination bonds, although no change in the macrocyclic complex structure of the support is observed; the saddle-shaped Fe TCPP may be placed on the ZnS surface in a single layer during immobilization,<sup>29</sup> resulting in the violet shift of the Soret peak.

The FT-IR spectrum of ZnS is similar to that of Fe TCPP/ZnS (Fig. 3). Absorption peaks between 3410 and 3465  $\text{cm}^{-1}$  are due to OH groups on the ZnS surface.<sup>30</sup> In the FT-IR spectra of Fe TCPP/ZnS, peaks observed at 1107, 619, and 473  $\text{cm}^{-1}$  are assigned to Zn-S vibrations.<sup>30,31</sup> The peak observed at 1640  $\text{cm}^{-1}$  in the spectrum of ZnS shifted to 1624  $\text{cm}^{-1}$  upon Fe TCPP immobilization on ZnS. The peak at 1001  $\text{cm}^{-1}$  disappeared and two new absorption peaks were observed at 931 and 1193  $\text{cm}^{-1}$ . This result indicates that Fe TCPP is immobilized on ZnS by coordination bonds, *i.e.*, Zn-S-Fe, which strengthens the stretching vibration frequency of the S-Fe bond, is formed. We therefore suggest that Fe TCPP is immobilized on ZnS such that sulfur atoms use one of the electron pairs of sulfur ion to coordinate with an iron ion, thereby forming an Fe TCPP/ZnS complex.

### XPS analysis of Fe TCPP and Fe TCPP/ZnS

X-ray photoelectron spectroscopy (XPS) was applied to study the composition of elements on or near the surface of the Fe TCPP and Fe TCPP/ZnS (Fig. 4 and Table 1). From Fig. 4a, at least 3 types of C species are fitted with bands at 284.8 eV (90.1%), 286.8 eV (2.2%), and 288.8 eV (7.7%), are found on Fe TCPP, which attribute to the existing of C species in C-H, C-OH, and C=C, respectively.<sup>32-34</sup> In C 1s spectrum of Fe TCPP/ZnS, the binding energy (284.8 eV) of C 1s of C-H was the same as that (284.8 eV) of Fe TCPP. The binding energy of C 1s in the C-OH, and C=C was blue shift by 1.2 eV and 0.2 eV, and the percentage of C in C-OH and C=C increased from 2.2% and

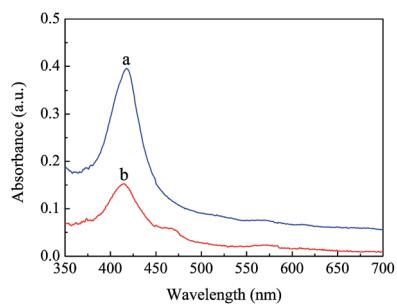


Fig. 2 UV-vis spectra at room temperature. Dimethyl formamide solution of Fe TCPP (a), suspension of Fe TCPP/ZnS in dimethyl formamide (b).

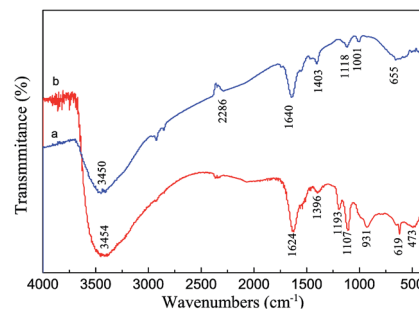


Fig. 3 FT-IR spectra of ZnS (a) and Fe TCPP/ZnS (b).

7.7% to 38.1% and 11.3%, respectively, which indicated that the chemical state of C might be affected by immobilizing on ZnS.

In the O 1s spectrum, the binding energy of O 1s in the Fe TCPP was 531.9 eV and 533.5 eV, respectively, which assigned to the carboxylic O (C=O) and hydroxyl O (C-OH).<sup>35</sup> In the Fe TCPP/ZnS, the binding energy of O 1s in hydroxyl (533.5 eV) and in carboxylic (531.9 eV) was slightly shifted to 533.3 eV and 531.7 eV, respectively. And the percentage of hydroxyl O was decreased from 52.2% to 9.1% as well as that of the carboxylic O was increased from 47.8% to 90.9%. However, after Fe TCPP immobilizing on ZnS. Meanwhile, to compare with the oxygen amounts of the two samples, which usually are represented by the XPS fitting peaks area,<sup>36</sup> the amount of carbonyl O is increased greatly and almost about double in the peak area to the one before Fe TCPP immobilizing on ZnS; and on the contrary, the amount of hydroxyl O is greatly reduced, and which is only 17% of the one before Fe TCPP immobilizing on ZnS. In general, the H readily ionized from C-OH to form free radicals, which lead to the change of the external environment of O in the C-OH. As shown in Table 1, the amount of C-OH is decreased, which means free radicals are easily formed and reacted after Fe TCPP immobilized on ZnS.

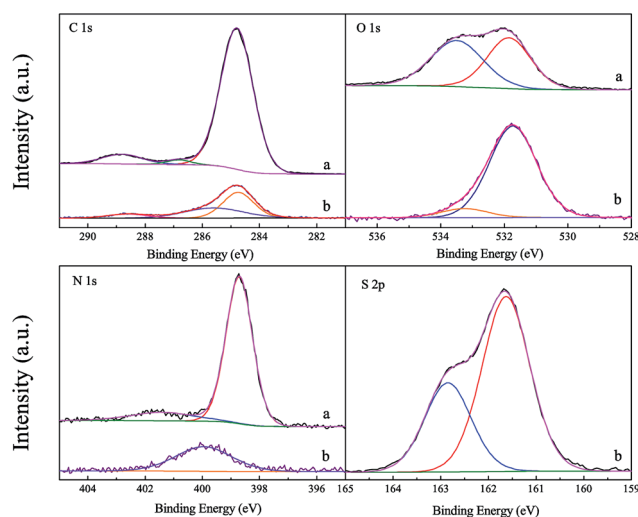


Fig. 4 XPS spectra of C 1s, O 1s, N 1s, and Fe 2p for Fe TCPP (a) and Fe TCPP/ZnS (b).

Table 1 Binding energy of core electrons of Fe TCPP and Fe TCPP/ZnS catalysts

XPS spectra	Existential form of elements	Fe TCPP			Fe TCPP/ZnS		
		BE/eV	Percent of valence state <sup>a</sup> /%	Peak area/unit	BE/eV	Percent of valence state/%	Peak area/unit
C 1s	C–H	284.8	90.1	67 148	284.8	50.6	11 619
	C–OH	286.8	2.2	1623	285.6	38.2	8761
	C=C	288.8	7.7	5731	288.6	11.3	2596
O 1s	C=O	531.9	47.8	18 448	531.7	90.9	35 845
	C–OH	533.5	52.2	20 117	533.3	9.1	3576
N 1s	N–Fe	398.7	88.1	8178			
	N–C	401.4	11.9	1105	400.1	100	2887
S 2p	S–Fe	—	—	—	161.6	66.9	25 716
	S–Fe	—	—	—	162.9	33.1	12 701

<sup>a</sup> Surface concentrations of different C, O, N, and S states are in parentheses.

The binding energy located at 398.7 eV and 401.4 eV in the N 1s spectrum of Fe TCPP are ascribed to the nitrogen in the Fe–N when Fe TCPP was formed and the pyrrolic nitrogen in the porphyrin core, respectively.<sup>37–39</sup> The results of N 1s spectrum of Fe TCPP indicate that there are at least two forms of nitrogen atoms in the Fe TCPP catalyst. The percentage of Fe–N is 88.1%, and the percentage of pyrrolic nitrogen is only 11.9% (Table 1). However, in the N 1s spectrum of the Fe TCPP/ZnS, only one characteristic peak located at 400.1 eV was observed and matches the contributions from the pyrrolic nitrogen in the porphyrin core, indicating the four equivalent nitrogen atoms in the complex.<sup>40,41</sup>

For S 2p XPS spectrum in the Fe TCPP/ZnS, the characteristic peaks of S 2p<sub>3/2</sub> and S 2p<sub>1/2</sub> are located at 161.6 eV and 162.9 eV, which are 161.9 eV and 163.2 eV in a pure ZnS.<sup>42</sup> After immobilization on ZnS, the binding energy of S 2p<sub>3/2</sub> and S 2p<sub>1/2</sub> blue shifted by 0.3 eV, respectively, which may be caused by the electronic interaction between the Fe ion and the ZnS substrate, indicating that coordination bonds (S–Fe) may be formed,<sup>43–45</sup> which reduced the redox potential of the Fe ion in Fe TCPP/ZnS. This results is helpful for oxygen activation by the metalporphyrin and improves the catalytic activity of the metalporphyrin.

### Effect of reaction conditions on Fe TCPP/ZnS-catalyzed cyclohexane oxidation

Fig. 5A shows the effect of reaction temperature on the cyclohexane oxidation reaction. When the temperature was below 160 °C, the cyclohexanone and cyclohexanol yields and turnover number (TON) increased quickly with increasing temperature. Cyclohexanone and cyclohexanol yields increased from 10.1% (145 °C) to 24.4% (160 °C) and TON increased from  $2.1 \times 10^5$  (145 °C) to  $8.6 \times 10^5$  (160 °C). However, at temperatures was higher than 160 °C, the TON, cyclohexane conversion, selectivity, and cyclohexanone and cyclohexanol yields decreased from  $8.6 \times 10^5$ , 64.9%, 37.6%, and 24.4% (160 °C) to  $3.7 \times 10^5$ , 54.9%, 25.1%, and 13.8% (165 °C), respectively. The decrease in cyclohexane conversion could be due to the low stability of the catalyst at higher temperatures, and the reduction in selectivity

at higher temperatures may be attributed to product oxidation.<sup>46</sup> In the present experiment, the optimal reaction temperature was 160 °C.

To determine whether or not higher pressures are beneficial to product yields, the effect of increasing pressure from 0.6 MPa to 1.0 MPa was investigated at 160 °C using Fe TCPP/ZnS as the catalyst; relevant results are shown in Fig. 5B. Cyclohexanone and cyclohexanol yields increased with increasing pressure and then decreased after a certain pressure was reached under the reaction conditions. Cyclohexanone and cyclohexanol yields were the highest (24.4%) when the pressure was 0.8 MPa. Higher oxygen pressures indicate higher initial dissolved oxygen concentrations in the liquid phase. After a certain

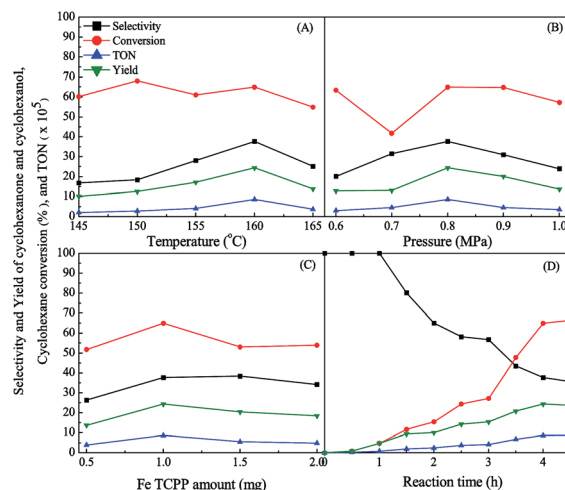


Fig. 5 Effects of reaction temperatures (A), reaction pressures (B), amount of Fe TCPP (C) and reaction time (D) on the cyclohexane oxidation catalyzed by Fe TCPP/ZnS. Reaction conditions: (A) cyclohexane, 200 mL; oxygen pressure, 0.8 MPa; Fe TCPP, 1.0 mg; reaction time, 4 h, tail gas flow,  $0.04 \text{ m}^3 \text{ h}^{-1}$ . (B) Cyclohexane, 200 mL; temperature, 160 °C; Fe TCPP, 1.0 mg; reaction time 4 h, tail gas flow,  $0.04 \text{ m}^3 \text{ h}^{-1}$ . (C) Cyclohexane, 200 mL; temperature, 160 °C; oxygen pressure, 0.8 MPa; reaction time, 4 h, tail gas flow,  $0.04 \text{ m}^3 \text{ h}^{-1}$ . (D) Cyclohexane, 200 mL; oxygen pressure, 0.8 MPa; temperature, 160 °C; Fe TCPP, 1.0 mg, tail gas flow,  $0.04 \text{ m}^3 \text{ h}^{-1}$ .

oxygen concentration is reached at 160 °C, further increases in oxygen pressure cannot markedly accelerate the reaction rate and cyclohexane conversion reaches nearly maximum values. Higher oxygen pressures in the reaction system can promote the formation of by-products, which are responsible for the low selectivities of cyclohexanone and cyclohexanol.<sup>10</sup> Catalysts can be destroyed by high oxygen concentrations,<sup>26</sup> thereby decreasing cyclohexane conversion. Based on the results, oxygen pressure is an important parameter influencing cyclohexane oxidation and 0.8 MPa is the optimal pressure promoting both activity and selectivity.

Fig. 5C shows that the optimal Fe TCPP value. As the Fe TCPP amount increased to 1.0 mg, maximum cyclohexanone and cyclohexanol yields were observed. Cyclohexanone and cyclohexanol yields subsequently decreased as the Fe TCPP amount continued to increase. Excessive addition of Fe TCPP may improve interactions between activated intermediates and suppress the formation of cyclohexanone and cyclohexanol.<sup>47</sup> The results indicate that the polymer microenvironment of metalloporphyrins catalysts is an important factor influencing product yields. This microenvironment not only facilitates catalytic action but also effectively protects metalloporphyrins from dimer formation and destruction, thereby resulting in high catalytic activity.<sup>16</sup>

Fig. 5D illustrates changes in the selectivity and yield of cyclohexanone and cyclohexanol, cyclohexane conversion, and TON under an optimal temperature of 160 °C and pressure of 0.8 MPa catalyzed by Fe TCPP/ZnS. In generally, yields increased with increasing reaction time. From 0 h to 0.5 h, cyclohexanone and cyclohexanol yields slightly increased. This phenomenon may be attributed to the fact that the supported catalyst undergoes induction and activation in the present reaction conditions and that cyclohexane is oxidized to only very small amounts of main products.<sup>10</sup> Cyclohexanone and cyclohexanol yields sharply increased after 4 h of reaction and then showed maxima (24.4%). Cyclohexanone and cyclohexanol selectivity decreased with increasing reaction time, possibly because these products are more readily oxidizable than cyclohexane. Besides the limited conversion observed, other oxidation products, such as adipic acid and ester, were observed. Fe TCPP/ZnS catalyzed cyclohexane oxidation under optimal conditions to give cyclohexanone and cyclohexanol with maximum yields (24.4%).

### Comparison of cyclohexane oxidation catalyzed by Fe TCPP/ZnS and Fe TCPP

To investigate the effect of ZnS on the cyclohexane oxidation reaction catalyzed by metalloporphyrins, the catalytic activities of Fe TCPP/ZnS and Fe TCPP were studied under the same conditions; relevant results are shown in Fig. 6.

Fe TCPP/ZnS exhibited more notable activities than Fe TCPP during cyclohexane conversion. When Fe TCPP/ZnS and Fe TCPP were used as catalysts after 4 h of reaction, cyclohexane conversion rates of 64.9% and 35.6%, respectively, were observed. These conversion rates indicate that interactions between ZnS and Fe TCPP enhance their catalytic activity during

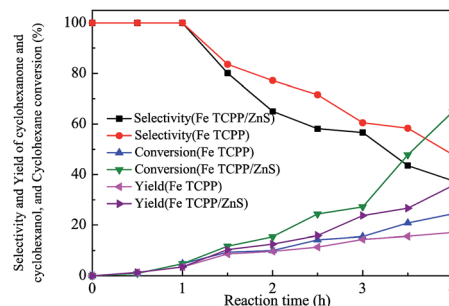


Fig. 6 Comparison of cyclohexane oxidation catalyzed by Fe TCPP/ZnS and Fe TCPP. Reaction conditions: cyclohexane, 200 mL; oxygen pressure, 0.8 MPa; temperature, 160 °C; Fe TCPP, 1.0 mg; reaction time, 4 h.

oxidation. When the chitosan-supported TPPFeCl,<sup>26</sup> Co<sup>II</sup> TPP/BM,<sup>25</sup> Co<sup>II</sup> TCPP/AlOOH,<sup>9</sup> Mn(III)TPP-Au/SiO<sub>2</sub>,<sup>48</sup> DP-IX-DME-Co(II),<sup>49</sup> and CTSPFe<sup>50</sup> Fe TNPP/BM,<sup>12</sup> and Fe T(*p*-MeO)PP/BM<sup>8</sup> was used as the catalyst, the cyclohexanone and cyclohexanol yields were 9.3%, 8.5%, 14.3%, 4.8%, 15.7%, 6.4%, 5.3%, and 4.7%, respectively. When ZnO was used as the support for Fe (TPFPP), the stability of the Fe (TPFPP) was improved, after reused for 11 times, the cyclohexanone and cyclohexanol yields just decreased from 22.5% to 18.1%.<sup>43</sup>

In the present study, the cyclohexanone and cyclohexanol yields reached 24.4% on Fe TCPP/ZnS, which was much higher than that of the previous studies. The reason is probably that the Fe TCPP/ZnS has a better performance for activating molecular oxygen than the Fe TCPP. And according to the results of UV-vis spectra and FT-IR spectra, the sulphur atom of ZnS may use one of the electron pairs to coordinate with a iron ion and cause the Fe TCPP immobilize on ZnS by chemical coordination, which may improve the activity of Fe TCPP. However, in the catalytic reaction process, Fe TCPP is superior to Fe TCPP/ZnS in promoting cyclohexanone and cyclohexanol selectivity. This result may be due to improvements in the catalytic activity of Fe TCPP when immobilized on ZnS, which increases the number of activated oxygen molecules. An abundance of activated oxygen molecules allows continuous oxidation of cyclohexanone and cyclohexanol to other by-products, such as acids and esters. In conclusion, ZnS is an excellent support that provides vital assistance for metalloporphyrins catalyzing cyclohexane oxidation.

### Cyclohexane oxidation catalyzed by reused Fe TCPP/ZnS

When Fe TCPP/ZnS is reused four times, cyclohexane conversion, cyclohexanone and cyclohexanol yields and TON remain higher than those obtained from Fe TCPP catalysis (Table 2). The Fe TCPP/ZnS results are attributed to the catalytic activity promotion of Fe TCPP by immobilization on ZnS, ZnS offers protection from destructive oxidation by oxygen,<sup>51</sup> prevents Fe TCPP agglomeration, and improves the mechanical strength of Fe TCPP, thereby rendering the Fe TCPP catalyst more stable, active, easily recoverable and reusable.

Table 2 Cyclohexane oxidation catalyzed by reused Fe TCPP/ZnS<sup>a</sup>

Catalysts	Run	Conversion/%	Selectivity/%	TON/(× 10 <sup>5</sup> )	Yield%
Fe TCPP/ZnS	1	64.9	37.6	8.6	24.4
	2	49.5	42.5	6.8	21.1
	3	40.9	46.8	5.8	19.2
	4	41.6	41.2	5.8	17.1
	Average	49.2	42.0	6.8	20.5
Fe TCPP	1	35.6	47.9	5.1	17.1

<sup>a</sup> Reaction conditions: cyclohexane, 200 mL; oxygen pressure, 0.8 MPa; temperature, 160 °C; Fe TCPP, 1.0 mg; reaction time, 4 h, tail gas flow, 0.04 m<sup>3</sup> h<sup>-1</sup>.

### Suggested mechanism for the cyclohexane oxidation catalyzed by Fe TCPP/ZnS

The catalytic oxidation reaction mechanism of metalporphyrin has recently been reported; metalporphyrin intermediates possess an important function in the oxidation reaction. Given current limitations in science and technology, many intermediates cannot be detected, so the reaction mechanism presented here is hypothetical.<sup>35</sup> Lyons<sup>36</sup> proposed a hypothetical catalytic oxidation hypothetical mechanism of iron porphyrins, which is similar to that of the P-450 enzyme. The reaction mechanism of cyclohexane oxidation catalyzed by Fe TCPP/ZnS is similar to that of hydrocarbon oxidation catalyzed by metalporphyrins, *i.e.*, a radical reaction mechanism. The suggested mechanism is shown in Fig. 7.

The suggested mechanism of cyclohexane oxidation catalyzed by Fe TCPP/ZnS is as follows: Fe<sup>III</sup> TCPP Cl/ZnS loses axial chlorine atoms and Fe<sup>III</sup> TCPP Cl/ZnS is reduced to Fe<sup>II</sup> TCPP/ZnS, which reacts with O<sub>2</sub> to form O<sub>2</sub>Fe<sup>III</sup>TCPP/ZnS. However, the peroxy bond of O<sub>2</sub>Fe<sup>III</sup>TCPP/ZnS is easily fractured, and [O=Fe<sup>IV</sup>TCPP/ZnS]<sup>+</sup> is generated. [O=Fe<sup>IV</sup>TCPP/ZnS]<sup>+</sup> intermediates show high activity for capturing hydrogen atoms of cyclohexane (RH) and form cyclohexyl radicals (R<sup>•</sup>), which causes the radical chain. After initiation of the radical chain, six radical chain transfer processes may occur according to eqn (1) to (6).

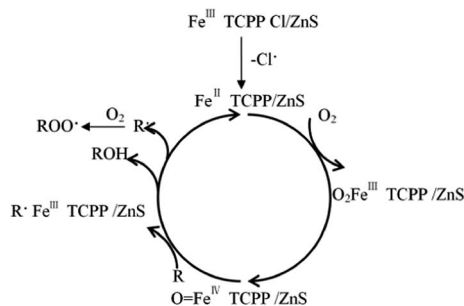
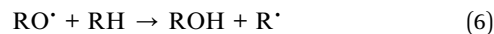
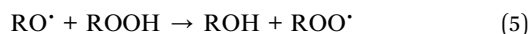


Fig. 7 Suggested mechanism of cyclohexane oxidation catalyzed by Fe TCPP/ZnS.



The radical chain stops when two cyclohexyl radicals collide, and radical coupling occurs to form R-R groups; two alkyl peroxy radicals (ROO<sup>•</sup>) may also react to form ketone (R=O) and oxygen. The catalytic mechanisms of supported and unsupported metalporphyrins are similar, but the redox potential of the Fe ion in Fe TCPP is fairly low because of the Zn-S-Fe bond formed between the Fe TCPP and ZnS, which was supported by the XPS results. The coordination bonds (S-Fe) promotes the catalysis of the Fe TCPP for the cyclohexane oxidation, which was similar to the results of our previous studies.<sup>43</sup> Therefore, the cyclohexane conversion, cyclohexanone and cyclohexanol yields can be improved by this process.

## Conclusions

ZnS promoted the catalytic activity of Fe TCPP for the aerobic oxidation of cyclohexane by forming coordination bonds with Fe TCPP. Under optimal conditions, the TON, cyclohexane conversion and cyclohexanone and cyclohexanol yields were 8.6 × 10<sup>5</sup>, 64.9%, and 24.4%, respectively. Fe TCPP/ZnS could continuously be reused four times in the aerobic oxidation of cyclohexane to cyclohexanol and cyclohexanone with little change of catalytic performance. The average cyclohexane conversion and cyclohexanone and cyclohexanol yields were 49.2% and 20.5%, respectively. ZnS significantly improved the catalytic activity of Fe TCPP for the aerobic oxidation of cyclohexane and is thus an excellent support material. Fe TCPP/ZnS catalyst, which possessed much higher catalytic activity than Fe TCPP, was conveniently prepared and was easily recovered by simple isolation from the reaction mixture, and it was a promising catalyst in industrial applications.

## Acknowledgements

This work was supported by the National Natural Science Foundation of China (no.: 51063001 and 51363001), the Guangxi Scientific and Technological Project (12118008-12-3), the Guangxi Natural Science Foundation (2012GXNSFAA053016 and 2014GXNSFDA118009) and the Open Project of Guangxi Key Laboratory of Petrochemical Resource Processing and Process Intensification Technology (2012K06).

## Notes and references

- J. Fischer, T. Lange, R. Boehling, A. Rehfinger and E. Klemm, *Chem. Eng. Sci.*, 2010, **65**, 4866–4872.
- B. P. C. Hereijgers and B. M. Weckhuysen, *J. Catal.*, 2010, **270**, 16–25.

- 3 F. C. Skrobot, I. L. V. Rosa, A. P. A. Marques, P. R. Martins, J. Rocha, A. A. Valente and Y. Yamamoto, *J. Mol. Catal. A: Chem.*, 2005, **237**, 86–92.
- 4 T. K. Chin, S. Endud, S. Jamil, S. Budagumpi and H. O. Lintang, *Catal. Lett.*, 2013, **143**, 282–288.
- 5 X.-T. Zhou, Q.-L. Yuan and H.-B. Ji, *Tetrahedron Lett.*, 2010, **51**, 613–617.
- 6 H. Chen, H. Ji, X. Zhou, J. Xu and L. Wang, *Catal. Commun.*, 2009, **10**, 828–832.
- 7 M. H. N. Olsen, G. C. Salomão, V. Drago, C. Fernandes, A. Horn Jr, L. C. Filho and O. A. C. Antunes, *J. Supercrit. Fluids*, 2005, **34**, 119–124.
- 8 M.-G. Fan, Z.-C. Luo, G. Huang, F. Xiang, Y.-A. Guo and H. Zhou, *J. Exp. Nanosci.*, 2013, **8**, 640–648.
- 9 G. Huang, L. Shen, Z.-C. Luo, Y.-D. Hu, Y.-A. Guo and S.-J. Wei, *Catal. Commun.*, 2013, **32**, 108–112.
- 10 C. Sun, B. Hu, D. Zhao and Z. Liu, *J. Appl. Polym. Sci.*, 2012, **125**, E79–E87.
- 11 X. Guo, D.-H. Shen, Y.-Y. Li, M. Tian, Q. Liu, C.-C. Guo and Z.-G. Liu, *J. Mol. Catal. A: Chem.*, 2011, **351**, 174–178.
- 12 G. Huang, Z.-C. Luo, F. Xiang, X. Cao, Y.-A. Guo and Y.-X. Jiang, *J. Mol. Catal. A: Chem.*, 2011, **340**, 60–64.
- 13 G. S. Machado, G. M. Ucoski, O. J. d. Lima, K. J. Ciuffi, F. Wypych and S. Nakagaki, *Appl. Catal., A*, 2013, **460–461**, 124–131.
- 14 G. S. Machado, G. G. C. Arizaga, F. Wypych and S. Nakagaki, *J. Catal.*, 2010, **274**, 130–141.
- 15 Q. Zhu, S. Maeno, M. Sasaki, T. Miyamoto and M. Fukushima, *Appl. Catal., B*, 2015, **163**, 459–466.
- 16 B. Gao, J. Zhao and Y. Li, *J. Appl. Polym. Sci.*, 2011, **122**, 406–416.
- 17 B. Fu, P. Zhao, H. C. Yu, J. W. Huang, J. Liu and L. N. Ji, *Catal. Lett.*, 2009, **127**, 411–418.
- 18 M. J. F. Calvete, M. Silva, M. M. Pereira and H. D. Burrows, *RSC Adv.*, 2013, **3**, 22774–22789.
- 19 M. Zhao, S. Ou and C.-D. Wu, *Acc. Chem. Res.*, 2014, **47**, 1199–1207.
- 20 S. Rayati, P. Jafarzadeh and S. Zakavi, *Inorg. Chem. Commun.*, 2013, **29**, 40–44.
- 21 M. Araghi and F. Bokaei, *Polyhedron*, 2013, **53**, 15–19.
- 22 X.-T. Zhou, H.-B. Ji and X.-J. Huang, *Molecules*, 2012, **17**, 1149–1158.
- 23 G. S. Machado, P. B. Groszewicz, K. A. D. D. F. Castro, F. Wypych and S. Nakagaki, *J. Colloid Interface Sci.*, 2012, **374**, 278–286.
- 24 G. M. Ucoski, K. A. D. D. F. Castro, K. J. Ciuffi, G. P. Ricci, J. A. Marques, F. S. Nunes and S. Nakagaki, *Appl. Catal., A*, 2011, **404**, 120–128.
- 25 G. Huang, T.-M. Li, S.-Y. Liu, M.-G. Fan, Y.-X. Jiang and Y.-A. Guo, *Appl. Catal., A*, 2009, **371**, 161–165.
- 26 C.-C. Guo, G. Huang, X.-B. Zhang and D.-C. Guo, *Appl. Catal., A*, 2003, **247**, 261–267.
- 27 N. Chauhan, J. Narang and C. S. Pundir, *Biosens. Bioelectron.*, 2011, **29**, 82–88.
- 28 M. Ghaedi, A. Ansari and R. Sahraei, *Spectrochim. Acta, Part A*, 2013, **114**, 687–694.
- 29 G. Huang, Z.-C. Luo, Y.-D. Hu, Y.-A. Guo, Y.-X. Jiang and S.-J. Wei, *Chem. Eng. J.*, 2012, **195–196**, 165–172.
- 30 G. Murugadoss, *Particuology*, 2013, **11**, 566–573.
- 31 R. John and S. Sasiflorence, *Chalcogenide Lett.*, 2010, **7**, 269–273.
- 32 P. Sundberg, R. Larsson and B. Folkesson, *J. Electron Spectrosc. Relat. Phenom.*, 1988, **46**, 19–29.
- 33 N. M. Mackie, D. G. Castner and E. R. Fisher, *Langmuir*, 1998, **14**, 1227–1235.
- 34 S. Ershov, F. Khelifa, V. Lemaure, J. Cornil, D. Cossement, Y. Habibi, P. Dubois and R. Snyders, *ACS Appl. Mater. Interfaces*, 2014, **6**, 12395–12405.
- 35 L. Kalina, J. Másilko, J. Koplík and F. Šoukal, *Cem. Concr. Res.*, 2014, **66**, 110–114.
- 36 Z.-Z. Qin, T.-M. Su, Y.-X. Jiang, H.-B. Ji and W.-G. Qin, *Chem. Eng. J.*, 2014, **242**, 414–421.
- 37 S. Xu, Z. Li, Y. Ji, S. Wang, X. Yin and Y. Wang, *Int. J. Hepatol.*, 2014, **39**, 20171–20182.
- 38 M. Lipińska, S. H. Rebelo and C. Freire, *J. Mater. Sci.*, 2014, **49**, 1494–1505.
- 39 J.-W. Huang, Z.-L. Liu, X.-R. Gao, D. Yang, X.-Y. Peng and L.-N. Ji, *J. Mol. Catal. A: Chem.*, 1996, **111**, 261–266.
- 40 S. Watcharinyanon, C. Puglia, E. Göthelid, J.-E. Bäckvall, E. Moons and L. S. O. Johansson, *Surf. Sci.*, 2009, **603**, 1026–1033.
- 41 M. E. Lipinska, J. P. Novais, S. L. H. Rebelo, B. Bachiller-Baeza, I. Rodriguez-Ramos, A. Guerrero-Ruiz and C. Freire, *Polyhedron*, 2014, **81**, 475–484.
- 42 P. Guo, J. Jiang, S. Shen and L. Guo, *Int. J. Hydrogen Energy*, 2013, **38**, 13097–13103.
- 43 G. Huang, L.-Q. Mo, J.-L. Cai, X. Cao, Y. Peng, Y.-A. Guo and S.-J. Wei, *Appl. Catal., B*, 2015, **162**, 364–371.
- 44 D. Brion, *Appl. Surf. Sci.*, 1980, **5**, 133–152.
- 45 B. A. Kwentkus, K. Sattler and H. Künzli, *Appl. Surf. Sci.*, 1993, **68**, 139–147.
- 46 A. Ebadi, N. Safari and M. H. Peyrovi, *Appl. Catal., A*, 2007, **321**, 135–139.
- 47 R. Wang, H. Zhu and B. Gao, *React. Kinet., Mech. Catal.*, 2011, **103**, 431–441.
- 48 J. Xie, Y. J. Wang and Y. Wei, *Catal. Commun.*, 2009, **11**, 110–113.
- 49 D. Ma, B. Hu and C. Lu, *Catal. Commun.*, 2009, **10**, 781–783.
- 50 G. Huang, C.-C. Guo and S.-S. Tang, *J. Mol. Catal. A: Chem.*, 2007, **261**, 125–130.
- 51 G. Huang, F. Xiang, T.-M. Li, Y.-X. Jiang and Y.-A. Guo, *Catal. Commun.*, 2011, **12**, 886–889.